Continuum States of the Hydrogen Molecule with the R-Matrix Method

JONATHAN TENNYSON* AND C. J. NOBLE

SERC, Daresbury Laboratory, Daresbury, Warrington WA4 4AD, UK

P. G. BURKE

*Department of Applied Mathematics and Theoretical Physics, The Queen's University of Belfast,
Belfast BT7 1NN, UK*

Abstract

The interaction of low-energy electrons with H_2^+ and light with H_2 is analyzed using the R-matrix method including both coupled state and polarization effects ab initio. Particular attention is paid to the energy region containing low-lying H_2^* resonances which converge to H_2^+ $A\,^2\Sigma_u^+$. Resonances in both elastic scattering and the photoionization asymmetry parameter, β, are presented. At low photon energies, satisfactory results for vibrationally resolved photoionization are obtained using the adiabatic nuclei approximation. The use of nonadiabatic techniques for higher energies is discussed.
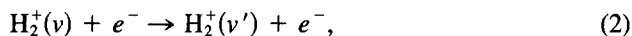
1. Introduction

Many fundamental processes involve the interaction of molecules with electrons and light. Even for simple hydrogenic systems these processes are not well understood because, in part, of long-lived resonances corresponding to localized excited states of H_2 lying in the continuum. The lowest of these resonances are those associated with the infinite Rydberg series which converges to the repulsive $A\,^2\Sigma_u^+$ state of H_2^+ (see Fig. 1).
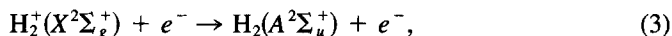
Such resonance effects are important for processes involving elastic scattering,

$$H_2^+ + e^- \rightarrow H_2^+ + e^-, \tag{1}$$

vibrational excitation,

$$H_2^+(v) + e^- \rightarrow H_2^+(v') + e^-, \tag{2}$$

electronic excitation,

$$H_2^+(X\,^2\Sigma_g^+) + e^- \rightarrow H_2(A\,^2\Sigma_u^+) + e^-, \tag{3}$$

dissociative recombination,

$$H_2^+ + e^- \rightarrow H + H, \tag{4}$$

---

*From October 1985: Department of Physics and Astronomy, University College London, London WC1E 6BT, UK.
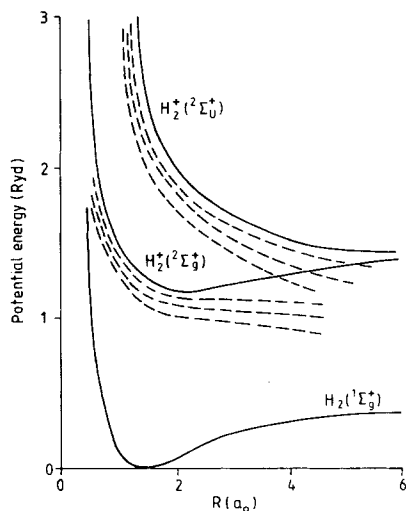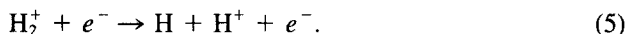
Figure 1. Potential curves for H_2 and H_2^+. The dashed lines illustrate schematically H_2^* Rydberg states converging to $H_2^+(X^2\Sigma_g^+)$ and $H_2^+(A^2\Sigma_u^+)$.
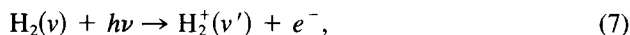
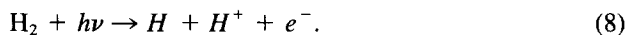and dissociative scattering (three-body dissociation),

$$H_2^+ + e^- \rightarrow H + H^+ + e^-. \tag{5}$$

Similarly, the interaction of molecular hydrogen with low-energy photons (<35 eV) can lead to photodissociation,

$$H_2 + h\nu \rightarrow H + H, \tag{6}$$

vibrationally resolved photoionization,

$$H_2(v) + h\nu \rightarrow H_2^+(v') + e^-, \tag{7}$$

and dissociative photoionization,

$$H_2 + h\nu \rightarrow H + H^+ + e^-. \tag{8}$$

Other possible exit channels include ones leading to ion pair formation, $H^+ + H^-$. These are, however, formed by curve crossings from the neutral dissociating species $H + H$ and will not concern us further here.

All the processes (1)–(8) go through common intermediates which are excited states (continuum states) of hydrogen, H_2^*. All the processes can thus be expected to show resonance effects due to localized H_2^* resonances. Furthermore, if any one process is studied, the others form competing exit channels which must also be taken into account in a full treatment. It is thus attractive to consider processes (1)–(8) using a common theoretical framework.

We have thus undertaken a systematic study of these using the R-matrix method. The fundamental nature of hydrogen makes it appropriate for such a study, although our methodology is directly transferable to molecules with more complicated electronic structures.

The basis of the current work is the two coupled-state, low-energy electron-H_2^+ scattering calculations by Tennyson and Noble [1, 2]. In this paper we review progress in utilizing these calculations for both electron and light scattering reactions. We present the first molecular photoionization calculations obtained with R-matrix method of Burke, Mackey, and Shimamura [3]. The need to extend the treatment of nuclear motion beyond the Born–Oppenheimer approximation and the complicated nature of the resulting nuclear motion problem is discussed.

2. Theory

The basis of the R-matrix method is the division of configuration space into internal and external regions. While interactions in the internal region can take any form, including for example electronic exchange, only simple (e.g., multipole) interactions are allowed in the external region. Figure 2 gives a schematic illustration of this division for the electronic problem.

Consider first electron scattering within a finite R-matrix sphere of radius a. The wave function for the kth state of $e - H_2^+$ within a two-state approximation is written

$$\Psi_k(\mathbf{x}_1, \mathbf{x}_2; R) = \mathscr{A} \sum_{i=1}^{2} \sum_j c_{ij}^k \phi_i(\mathbf{x}_1) F_{ij}(\mathbf{x}_2) + \sum_i b_i^k \phi_i(\mathbf{x}_1, \mathbf{x}_2), \tag{9}$$

where $\mathbf{x}_i$ represents the space-spin coordinates of the ith electron and $\mathscr{A}$ antisymmetrizes the scattered and target electrons.

The two target states retained in the close-coupling expansion correspond to the ground $X^2\Sigma_g^+$ and first excited $A^2\Sigma_u^+$ states of H_2^+ (see Fig. 2). These were represented by LCAO-SCF-MO wave functions constructed from $(2s, 1p)$ STO's on each H. These functions are assumed to have zero amplitude on the R-matrix boundary for which $a = 10a_0$ was used. The continuum orbitals, F_{ij}, which carry the scattering electron, were generated numerically to give a complete set for a suitable model problem for a given energy range ($E \leq 11$ Ryd) (see Ref. 1 for details).

The last term in expansion (9) consists of L^2 configurations constructed from the target MO's. Two models were used by Tennyson and Noble. The simple close-coupling (CC) or static exchange model accounts for short-range, high-angular-momentum effects which would otherwise be neglected in the truncation of the
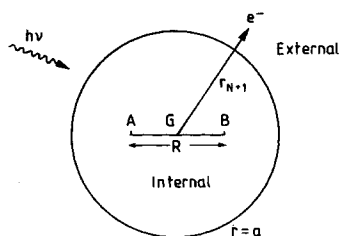

Figure 2. Schematic representation of the electronic R-matrix regions for diatomic AB with center of mass G.

partial wave expansion to $l \leq 6$ by including those configurations which freeze the target electron in either the $1\sigma_g$ or $1\sigma_u$ orbital. Polarization effects neglected in the truncated close-coupling expansion are included in the close-coupling plus correlation (CCC) model by allowing both electrons to occupy any target virtual orbital, subject only to symmetry constraints. All results presented here used the CCC model.

Once the variational problem implied by (9) has been solved, the R-matrix can be constructed on the R-matrix boundary [3]

$$R_{ij}(E) = \frac{1}{2a} \sum_k \frac{w_{ik}(a)w_{jk}(a)}{E_k - E},\tag{10}$$

where E is the energy of the scattered electron and E_k the energy of Ψ_k. The reduced boundary amplitude of the ith asymptotic channel contributed by the kth state is given by w_{ik}, which is computed by summing over the contribution of the continuum functions, F. As these functions are constructed using fixed boundary conditions [1], a Buttle correction [4] is added to the diagonal elements of $\mathbf{R}$. Solutions of the scattering problem are obtained by solving for $\mathbf{R}$ using standard techniques [5].

The effects of nuclear motion can be included within this formalism by generalizing the electronic R-matrix (10). Taking the kth R-matrix pole as a function of H_2^+ internuclear separation R, one can obtain the jth solution for a nuclear motion problem with $A_{in} \leq R \leq A_{out}$, $\theta_{jk}(R)$. The generalized electronic R-matrix can then be written

$$R_{iv, i'v'}(E) = \frac{1}{2a} \sum_{jk} \frac{\gamma_{ivjk}(a)\gamma_{i'v'jk}(a)}{E_{jk} - E},\tag{11}$$

where E_{jk} is the energy of state θ_{jk}. In the case where none of the R-matrix curves cross, the generalized amplitudes can be written

$$\gamma_{ivjk}(a) = \langle \zeta_{iv} \mid \theta_{jk}w_{ik}(a)\rangle,\tag{12}$$

where ζ_{iv} is the wave function of the vth vibrational state of the target electronic state associated with asymptotic channel i. The integral in (12) is over R between A_{in} and A_{out}, which are chosen such that

$$\zeta_{iv}(A_{in}) = \zeta_{iv}(A_{out}) = 0, \qquad \theta_{jk}(A_{in}) = 0.\tag{13}$$

Similar R matrices for the nuclear dissociative channels can be constructed [6]. This R-matrix theory has been extended to the case of isolated curve crossings [6] and used for vibrational excitation calculations on N_2 [7].

3. Low-Energy Electron Scattering

Calculations on the elastic scattering, process (1), of low-energy electrons from H_2^+ for both two- and four-state close-coupling approximations have been performed by Tennyson and Noble [2]. The explicit inclusion of the first excited state in the close-coupling expansion allows an arbitrary number of resonances belonging to the Rydberg series which converges to this state to be resolved (see Fig. 3).

Tennyson and Noble undertook a systematic of $e - H_2^+$ scattering for Σ and Π symmetries as a function of H_2^+ bondlength [2]. Comparison of their resonance poten-
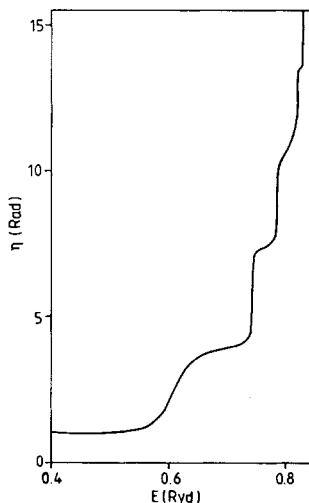
Figure 3. Eigenphase, η, for elastic e—H_2^+ scattering with $^1\Sigma_u^+$ symmetry and $R = 2.0a_0$. The lowest five Rydberg resonances are resolved.

tial energy curves and resonance widths with the results of other calculations revealed certain discrepancies in other theoretical treatments. In particular, one-state scattering calculations which included channel-coupling effects purely via an optical potential [8] were found not to always give reliable results for higher resonances. Furthermore, resonance widths for the important, especially for dissociative recombination process (4), $^1\Sigma_g^+$ symmetry for previous scattering calculations had the wrong behavior at large R. Recent scattering calculations by Hara and Sato [9] attribute this to the neglect of angular correlation effects.

Coupled-states calculations also allow electronically inelastic effects to be calculated. Figure 4 shows cross sections for the electronic excitation of H_2^+, process (3). As the $A^2\Sigma_u^+$ potential energy curve is dissociative, cross sections are actually for the fixed nuclei approximation to the dissociative scattering process (5). The large cross section at 1.0 Ryd is caused by a resonance in the $^3\Sigma_u^+$ symmetry. This resonance is a member of the Rydberg series which converges to the second excited, $B^2\Pi_u$, state of H_2^+.

4. Photoionization

Within the dipole length approximation, the photoionization cross section can be written [11]

$$\frac{d\sigma^L}{d\Omega} = 4\pi^2\alpha a_0^2\omega \, |\langle \Psi_E^{(-)}|\boldsymbol{\varepsilon} \cdot \mathbf{D}^L|\Psi_0\rangle|^2, \tag{14}$$

which, when averaged over molecular orientation and spin, gives

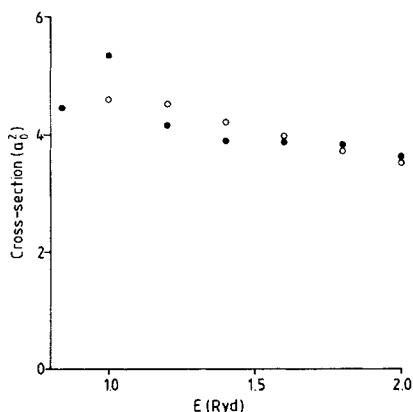$$\left(\frac{d\sigma^L}{d\Omega}\right)_{Av} = \frac{\sigma}{4\pi}[1 + \beta P_2(\cos\theta)], \tag{15}$$

Figure 4. Total excitation cross section $^2\Sigma_g^+ \rightarrow {}^2\Sigma_u^+$ for $e - H_2^+$ scattering with $R = 2a_0$. (●) Tennyson and Noble, two-state CCC [2]; (○) Collins and Schneider, two-state CC [10].

where θ is the angle between the polarization vector ε of the photon, which has frequency ω, and the ejected electron. Ψ_0 is the wave function of the hydrogen target. So as to minimize systematic errors, we follow atomic R-matrix calculations [12] and obtain Ψ_0 by performing a scattering calculation analagous to that used to obtain Ψ_E, but at a negative scattering energy. Such a bound-state calculation for H_2 at its equilibrium separation, $R = 1.4a_0$, gave an energy of $-1.1695E_h$ which means that 90% of correlation energy was recovered.

The minus superscript on $\Psi_E^{(-)}$ in Eq. (14) denotes that it has been transformed to half-scattering boundary conditions. The dipoles were obtained by computing dipole matrix elements in the internal region for the terms in expansion (9). These were calculated using a modified version of the ALCHEMY electronic structure package [13]. The dipoles are then summed over the coefficients of the bound and scattering wave functions. The full transition dipoles were actually constructed following the matrix formulation of Burke and Taylor [14]. They were found to be in surprisingly good agreement, considering the differences in numerical procedures, with the transition dipoles computed for the photoionization of H_2 by Flannery and Opik [15].

Figure 5 gives calculated values of the asymmetry parameter, β, for two H_2 geometries. Both curves show pronounced resonances for photon energies above 28 eV. These resonances, which have recently been predicted by Raseev [16], are due to the temporary formation of resonant states of H_2^*. These states are sufficiently long lived for information on the initial photon to be lost before autoionization occurs, resulting in sharp decreases in β.

The position of the resonances show a strong dependence on H_2^+ geometry. This means that any full understanding of this process must include the effects of nuclear motion.

In the adiabatic nuclei approximation the two steps of the Born–Oppenheimer approximation are treated separately. Vibrationally resolved photoionization cross sections can then be obtained by vibrationally averaging the transition dipoles
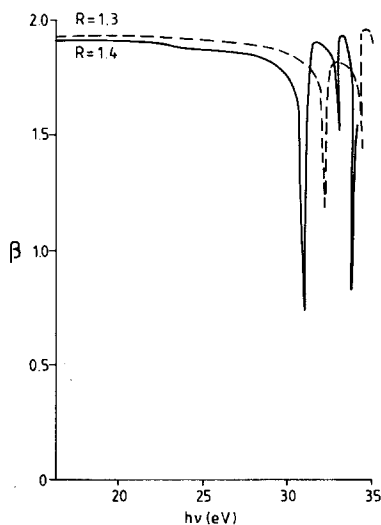
Figure 5. Asymmetry parameter, β, as a function of photon energy for two typical H_2 geometries.

$\langle \psi_E^{(-)} | D | \psi_0 \rangle$. Within the R-matrix method, this is equivalent to assuming that the internal R-matrix curves do not cross and that all solutions of the internal nuclear motion problem, θ_{jk}, are degenerate, i.e., $E_k \simeq E_{jk}$.

Tables I and II compares our values for vibrationally resolved cross sections and asymmetry parameters with previous results for the He II line at 584 Å (21.2 eV). The theoretical treatments all rely on the adiabatic nuclei approximation. It can be seen that the results are in good agreement and that for this energy, which is below the resonance region, the adiabatic nuclei approximation appears to work well.

Figure 6 shows our vibrationally resolved β parameters as a function of photon wavelength. Two trends are noticeable: an increase in β with vibrational state of the ion, and a decrease in β with increasing photon energy. The break in the curve for the H_2^+ vibrational ground state at about 22 eV corresponds the start of the resonance region.

TABLE I. Relative intensity, $\sigma(v')/\sigma(v' = 2)$, for the 584-Å line for $H_2(v = 0) + h\nu \rightarrow H_2^+(v') + e^-$ (absolute values in a.u. in parenthesis).

v'	Theory			Experiment	
	Ref. 17	Ref. 18	This work	Ref. 19	Ref. 20
0	0.467	0.465	0.446	0.438	0.434
1	0.874	0.873	0.868	0.850	0.839
2	(0.0386)	(0.0340)	(0.0387)	(0.0374)	
3	0.916	0.919	0.916	0.946	0.937
4	0.736	0.751	0.746	0.783	0.778
5	0.556	0.575	0.569	0.595	0.593

TABLE II. Asymmetry parameters, $\beta_{v'}$, for the 584 Å line for H_2 · $(v = 0) + h\nu \rightarrow H_2^+(v') + e^-$ (experimental errors in the last digit in parenthesis).

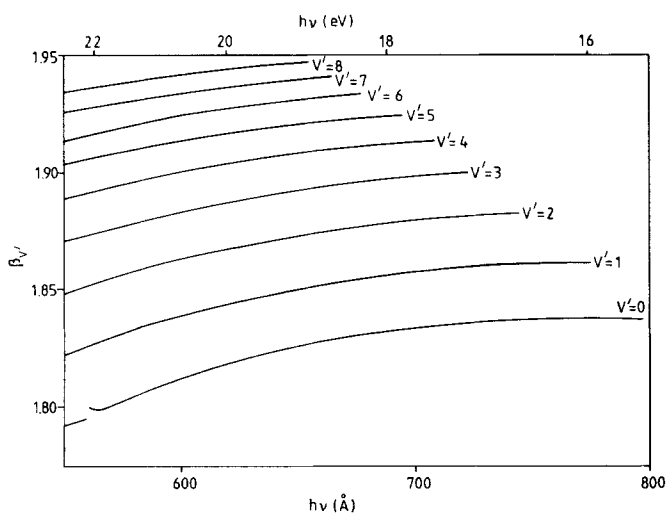| v'	Theory			Experiment[a]	
	Ref. 17	Ref. 18	This work	Ref. 19	Ref. 20
0	1.797	1.891	1.807	1.868(14)	1.862(19)
1	1.843	1.904	1.835	1.878(11)	
2	1.873	1.917	1.859	1.899(9)	
3	1.895	1.929	1.880	1.918(8)	
4	1.912	1.938	1.897	1.923(8)	
5	1.925	1.945	1.911	1.933(8)	

[a]As deduced by Sato and Ogata Ref. 18.

Figure 6. Vibrationally resolved asymmetry parameter, $\beta_{v'}$, as a function of photon energy.

5. Beyond the Adiabatic Approximation

In the resonance region the adiabatic nuclei approximation is no longer valid. This is because the Franck–Condon-like factors which couple initial and final vibrational states are destroyed by the formation of intermediate resonance states whose lifetimes are sufficient for several vibrations to occur before autoionization. Alternatively, the approximation that the θ_{jk} are degenerate for all j is not valid in a region where the electron scattering energy is close to the R-matrix poles, E_{jk}.

It is thus necessary, for both electron scattering processes (1)–(5) and light driven processes (6)–(8), to move beyond the adiabatic nuclei approximation in the resonance region. This requires a more detailed consideration of the R-matrix poles. Figure 7 depicts the lowest twenty R-matrix pole positions for $e - H_2^+$ scattering with $^1\Sigma_u^+$ symmetry, as a function of bond length. The picture is clearly complicated, with
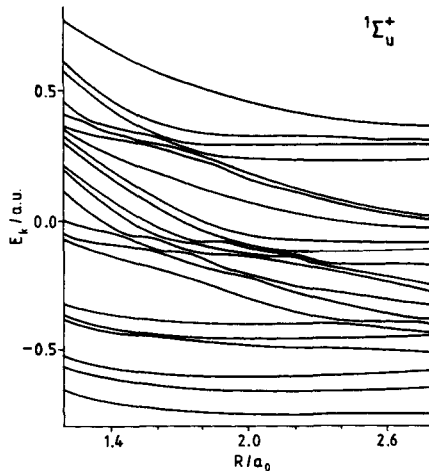
Figure 7. Lowest twenty R-matrix pole positions, E_k, for e — H_2^+ scattering with $^1\Sigma_u^+$ symmetry, as a function of internuclear separation.

many narrowly avoided crossings and several strongly avoided ones. This pattern of crossings can be attributed to the intersection of curves which follow the ground state of H_2^+ with those following the repulsive first excited state of H_2^+. This behavior is similar to that of the H_2 Rydberg states with these convergence limits, whose behavior is given schematically in Figure 1. This complicated picture cannot easily be treated within the simple isolated crossing model of Schneider, Le Dourneuf, and Burke [6].

Furthermore, many of the curves shown in Figure 7 are dissociative. Calculations on e — F_2 scattering have shown that if channels associated with the dissociative attachment process

$$F_2 + e^- \rightarrow F + F^- \tag{15}$$

are omitted, spurious resonance effects are observed in the vibrational excitation cross sections [21].

A method which will allow us to treat vibrational excitation and vibrationally resolved photoionization for the states of H_2^* lying in the continuum is currently being developed. Results will be reported elsewhere.

Bibliography

[1] J. Tennyson, C. J. Noble, and S. Salvini, J. Phys. B **17**, 905 (1984).

[2] J. Tennyson and C. J. Noble, J. Phys. B **18**, 155 (1985).

[3] P. G. Burke, I. Mackey, and I. Shimamura, J. Phys. B **10**, 2497 (1977).

[4] P. J. A. Buttle, Phys. Rev. **160**, 719 (1967).

[5] C. J. Noble and R. K. Nesbet, Comput. Phys. Commun. **33**, 4 (1984).

[6] B. I. Schneider, M. Le Dourneuf, and P. G. Burke, J. Phys. B **12**, L365 (1979).

[7] M. Le Dourneuf, Vo Ky Lan, and B. I. Schneider, in *Electron-Atom and Molecule Collisions*, J. Hinze, Ed. (Plenum, New York, 1983).

[8] H. Tagaki and H. Nakamura, Phys. Rev. A **27**, 691 (1983).

[9] S. Hara and H. Sato, J. Phys. B **17**, 4301 (1984).

[10] L. A. Collins and B. I. Schneider, Phys. Rev. A **27**, 101 (1983).

[11] P. G. Burke, in *Atomic and Molecular Collision Theory*, F. A. Gianturco, Ed. (Plenum, New York, 1982) p. 69.

[12] P. C. Ojha and P. G. Burke, J. Phys. B **16**, 3513 (1983).

[13] C. J. Noble and R. K. Nesbet, program TMT.

[14] P. G. Burke and K. T. Taylor, J. Phys. B **8**, 2620 (1975).

[15] M. R. Flannery and U. Öpik, Proc. Phys. Soc. **86**, 491 (1965).

[16] G. Raseev, J. Phys. B **18**, 423 (1985).

[17] Y. Itikawa, H. Tagaki, H. Nakamura, and H. Sato, Phys. Rev. A **27**, 1319 (1983).

[18] S. Hara and S. Ogata, J. Phys. B **18**, L59 (1985).

[19] J. E. Pollard, D. J. Trevor, J. E. Reutt, Y. T. Lee, and D. A. Shirley, J. Chem. Phys. **77**, 34 (1982).

[20] M.-W. Ruf, T. Bregel, and H. Hotop, J. Phys. B **16**, 1549 (1983).

[21] L. A. Morgan, to be published.